Title
Expression, Purification and Crystallization Studies of Lactose Permease Mutants

Author
Bajaj, Renata Alexandra

Publication Date
2014

Peer reviewed|Thesis/dissertation

UNIVERSITY OF CALIFORNIA

Los Angeles

Expression, Purification and Crystallization Studies of Lactose Permease Mutants

A thesis submitted in partial satisfaction of the requirements for the degree of Master of Science in Physiological Science

By

Renata Alexandra Bajaj

2014

ABSTRACT OF THE THESIS

Expression, Purification and Crystallization Studies of Lactose Permease Mutants

by

Renata Alexandra Bajaj

Master of Science in Physiological Science

University of California, Los Angeles 2014

Professor Barnett A. Schlinger, Chair

Lactose permease (LacY) catalyzes oligosaccharide/H^+ symport across the membrane. Until recently, all LacY structures demonstrate inward-open conformations with closed periplasmic side. We sought to obtain LacY crystals that diffract at higher resolution and/or provide previously unsolved conformation. The strategy was to employ hybrid proteins available in the laboratory in which cytochrome$_{b562}$ or flavodoxin-1 of *E. coli* was fused to LacY. Of the sixteen constructs, large-scale expression/purification of two LacY/cytochrome$_{b562}$ constructs was successful but crystallization proved difficult.

The crystal structure of LacY double-Trp (G46W/G262W) mutant with β-D-galactopyranosyl-1-thio-β-D-galactopyranoside (TDG) was recently reported. This structure has almost occluded, outward-open conformation with a rotation at the thioester linkage in TDG as compared to the previous structures. We obtained crystals of this double-mutant with octyl β-D-galactopyranoside that diffracted to ~20 Å. A mutagenesis strategy is proposed to obtain LacY in fully outward-open conformation. Further, a transport mechanism involving a configurational change(s) in TDG is postulated.

Pascal F. Egea

Alan D. Grinnell

Barnett A. Schlinger, Committee Chair

University of California, Los Angeles

2014

TABLE of CONTENTS

LIST OF FIGURES

ACKNOWLEDGMENTS

This work was performed using the UCLA facilities of the Department of Physiology LacY laboratory (Director Dr. Ronald Kaback), Department of Biological Chemistry membrane structural biology laboratory (Director Dr. Pascal Egea) and Molecular Biology Institute — Protein Expression Technology Center (Director Dr. Mark Arbing), Crystallization Core Facility (Director Michael Collazo), and X-ray Facility (Director Dr. Duilio Cascio). I thank each one of the aforementioned faculty for his valuable guidance and support.

I also wish to thank Dr. Gil Prive for providing the LacY chimeric permease constructs. In addition, I wish to thank Dr. Barney Schlinger, Dr. Egea, and Dr. Alan Grinnell for being members of my Master's Thesis committee and for their time, guidance, support and encouragement during this process.

I am especially grateful to Dr. Egea and Dr. Cascio for extensive involvement and guidance in experimental strategies and execution, as well as Dr. Lorena Saelices for data collection at the Advanced Photon Source.

Finally, I thank Mike Carr in the Department of Integrative Biology and Physiology, and Debra Moorehead and Carolina Dominguez in the Department of Physiology for their administrative support.

INTRODUCTION

Transport proteins are part of integral membrane proteins in which the major facilitator superfamily (MFS) (Griffith *et al*., 1992; Baldwin, 1993; Goswitz and Brooker, 1995; Pao *et al*., 1998; Saidijam *et al*., 2011; Saier *et al*., 1999; Saier, 2000; Reddy *et al*., 2012; Madej *et al*., 2013; Madej and Kaback, 2013) and ATP-binding cassette (ABC) superfamily (Higgins, 1992; Fath and Kolter 1993; Island and Kadner, 1993; Dean and Allikmets, 1995a,b; Dean *et al*., 2001; Higgins, 2001) are found to occur ubiquitously in all classifications of living organisms (Pao *et al.*, 1998; Paulsen *et al*., 1998; Saier *et al*., 1999; Saier 2000; Reddy *et al*., 2012; Madej *et al*., 2013; Madej and Kaback, 2013). The MFS proteins transduce the free energy stored in an electrochemical proton gradient into a substrate concentration gradient (Madej *et al*., 2013; Reddy *et al*., 2012), whereas the ABC superfamily utilizes the energy released from ATP hydrolysis to drive solute accumulation or efflux (Island and Kadner, 1993; Higgins, 2001). Members of the ABC superfamily are multicomponent transporters capable of transporting both small molecules and macromolecules, and are referred to as primary transporters (Higgins, 1992; Paulsen *et al*., 1997; Higgins, 2001). On the other hand, members of the MFS superfamily are single-polypeptide transporters capable of transporting only small molecules and are referred to as secondary transporters (Pao *et al*., 1998; Reddy *et al*., 2012; Madej *et al*., 2013).

The MFS represents the largest and most diverse group of transporters in the membranes of all living cells, and constitute ~25 % of prokaryotic membrane transport proteins (Paulsen *et al*., 1998; Saier *et al*., 1999; Saier, 2000; Reddy *et al*., 2012). They

are also referred to as the uniporter-symporter-antiporter family and transport a wide range of substrates in both directions across the membrane (Baldwin, 1993; Goswitz and Brooker, 1995; Pao *et al*., 1998; Madej *et al*., 2013). MFS transporters mostly contain 12 irregular transmembrane helices that form a deep central hydrophilic cavity through which the substrate/ions are transported (Calamia and Manoil, 1990; Abramson *et al*., 2003; Guan and Kaback, 2006; Dang *et al*., 2010; Madej *et al*., 2013). This family of proteins likely evolved from intragenic multiplication (Pao *et al*., 1998; Hvorup and Saier, 2002) since they share an alternating inverted triple-helix structural symmetry within the N- and C- terminal six-helix bundles (Radestock and Forrest, 2011). Although, MFS transporters have similar structural features, they share only weak sequence identities. Further, an important feature of the secondary transporters is their conformational adaptabilities to access the sugar from either side of the membrane without significantly altering the sugar and proton binding sites (Radestock and Forrest, 2011; Smirnova *et al*., 2011; Sugihara *et al*., 2012).

The lactose permease (LacY) of *E. coli* is the most extensively studied MFS protein (Guan and Kaback, 2006; Smirnova *et al*., 2011) and is part of the oligosaccharide:H^+ symporter (OHS) family (Pao *et al*., 1998). LacY catalyzes the symport of D-galactose and D-galactopyranoside with an H^+ across the membrane in either direction, depending upon the polarity of the sugar concentration gradient or the H^+ electrochemical gradient (Guan and Kaback, 2006; Madej and Kaback, 2014). Until recently, the structures of wild-type LacY (Guan *et al*., 2007), the conformationally restricted C154G mutant (Abramson *et al*., 2003; Mirza *et al*., 2006) and a single-Cys

mutant with a covalently bound inactivator (Chaptal *et al*, 2011) had been determined by X-ray crystallographic methods, and all of these structures exhibit the same inward-open conformation with a relatively low resolution. As predicted, the LacY monomer is composed of 12 transmembrane helices in which the N- and C-terminal six helices form two distinct helical bundles (Fig. 1). In all structures, LacY molecule has a large interior hydrophilic cavity tightly closed from the periplasmic side and open only from the cytoplasmic side, which represents an inward-facing conformation as illustrated in the report by Abramson *et al*., 2003. In the structure (Fig. 1), the β-D-galactopyranosyl-1-thio-β-D-galactopyranoside (TDG), a homolog of lactose, is located at roughly the same distances from both sides of the membrane (Abramson *et al*., 2003).

The exposed hydrophilic surface area of LacY is extremely small, which limits extensive crystal contacts that, in part, might contribute to obtaining the low resolution diffracting crystals. Our initial objective was to increase the hydrophilic surface area of LacY using the approach implemented successfully earlier for crystallization of the β2-adrenergic G-protein coupled receptor (GPCR) (Rosenbaum *et al*., 2007). For this, Rosenbaum and colleagues designed a chimeric GPCR consisting of a T4-lysozyme sequence (PDB ID 2LZM) inserted between helix 5 and 6 of the receptor, thereby stabilizing the two flexible helices and allowing the protein to crystallize more readily (Rosenbaum *et al*., 2007). For the first part of the proposed studies, we obtained putative hybrid molecules containing cytochrome$_{b562}$ or bacterial flavodoxin-1 insert (Fig. 2, Table 1) into several loops of LacY (Prive *et al*., 1994; Engel *et al*., 2002). Although attempts had been made earlier to crystallize these hybrid proteins without success, we wished to

employ the recent advancements in the membrane protein crystallization techniques to determine whether we could obtain crystals of the hybrid LacY molecules. DNA sequencing, expression/purification and crystallization trails of these hybrid molecules constitute the first part of the thesis.

Recently, crystal structure of a double-Trp mutant (G46W/G262W) of LacY was determined at 3.5 Å resolution in partially occluded, outward-open conformation with a bound lactose analog, TDG (Kumar *et al*., 2014). The TDG molecule in this structure (Fig. 3) has a different configuration and interacts more strongly with LacY than the previously published structure (Abramson *et al*., 2003). We attempted to obtain crystal structures of this double-Trp LacY mutant with octyl β-D-galactopyranoside ligand to understand if the galctopyranoside ring interacts similarly as in TDG. Initial screens yielded crystals that diffracted to ~20 Å. Additional crystallization trials and extensive resources would be required to obtain crystals with improved resolution. Further, based upon analysis of the double-Trp mutant, we provide a mutagenesis strategy to obtain structure of LacY in fully outward-open conformation. Finally, consistent with the available data, a configurational change in TDG during transport is proposed that has not been discussed or elaborated previously.

MATERIALS and METHODS

Preparation of Chemically Competent Escherichia coli Cells

Frozen *E. coli* competent cells (XL1 Blue, C41; see Table 2) were plated on Luria-Bertani (LB) agarose plates containing the appropriate antibiotics and incubated at 37 ˚C for 16 h. Single colonies were inoculated into 5-mL cultures LB broth containing the appropriate antibiotics and grown in incubator-shaker at 37 ˚C for 16 h. The 5-mL cultures were then diluted 10-fold into media of the same composition and grown to OD_{600nm} = 0.6. Cultures were centrifuged at 4000 rpm for 10 min and supernatants discarded. Cells were resuspended in 50 mM $CaCl_2$ on ice in half the original volume and incubated on ice for 30 min. The suspensions were then centrifuged at 4000 rpm for 10 min and supernatants again discarded. Cell pellets were resuspended in a solution containing 50 mM $CaCl_2$ and 15% glycerol in 10 percent of the original volume, flash frozen and stored at -80 ˚C.

Cloning and Construct Design

Lactose permease gene was cloned from *E. coli* genomic DNA into the pT7-5 expression vector, and carrier protein coding sequence was inserted at various sites of *lacY* sequence in previous studies (Engel *et al*., 2002). Competent *E. coli* XL1Blue cells were transformed with each plasmid of interest. Approximately 5 μg of DNA was incubated in 50 μL competent cells for 20 min on ice, 45 sec at 42 ˚C, followed by 5 min on ice. Cells were allowed to grow for one hour in standard outgrowth culture broth at 37

˚C while shaking, and the entire quantity of cells was plated on LB-agarose plates containing ampicillin (100 μg/mL) and incubated for 16 h at 37 ˚C. Single colonies were inoculated in 5 mL LB broth containing ampicillin (100 μg/mL) and incubated for 16 h at 37 ˚C. Single colonies were inoculated in 5 mL LB broth containing ampicillin (100 μg/mL) for 16 hours, cells were pelleted and the plasmid DNA was purified using the QIAGEN Miniprep kit (www.qiagen.com) and sequenced using the Sanger sequencing technology at the GenoSeq UCLA facility.

Construct Mutagenesis

For the chimeric permeases listed in Table 1, site-directed mutagenesis of residue Cys-154 to Gly-154 (C154G mutagenesis) was performed using the Quikchange method (Stratagene) with forward primer 5'-GCGCTGGGCGCCTCAATTGTCGGGATCATG-3' and reverse primer 3'-CATGATCCCGACAATTGAGGCGCCCAGCGC-5' (Integrated DNA Technologies) as outlined earlier (Smirnova *et al.*, 2003). The double-Trp LacY mutant was prepared as described in Smirnova *et al*., 2013.

Small Scale Expression Studies

Competent *E. coli* XL1Blue cells (Table 2) were transformed as described above. Colonies were inoculated into 25 mL cultures LB broth and grown to OD_{600nm} = 0.6 at 37 ˚C while shaking. Cultures were induced to 0.4 mM and 1.0 mM isopropyl β-D-1-thiogalactopyranoside (IPTG) and continued to grow in similar conditions for 4 h. Cells were harvested at 4000 rpm for 15 min; pellets were resuspended and washed in 50 mM

potassium phosphate (KP_i) pH 7.5 at 4000 rpm for 15 min. Cells were kept on ice at 4 ˚C for 16 h before small-scale membrane preparation as described below. Total membrane protein concentration was quantified using Pierce Micro-BCA analysis. Quantities of 2-40 µg total membrane protein were analyzed using SDS-PAGE and immunoblot (Western blot) analyses as described below.

Membrane Preparation

Cell pellets were resuspended in 5x volume of a refrigerated buffer containing 50 mM sodium phosphate (NaP_i) pH 7.5, 2 mM DTT, 28 mg/L DNAse (Calbiochem), 102 mg/L Pefabloc (Gold Biotechnology), and 15 mg/L Complete tablets (Roche Diagnostics) and lysed 2x at 1500-2000 psi in a French Pressure Cell. Cell debris was removed by centrifugation in a GSA rotor at 11,000 rpm x15 min. Supernatant was then ultracentrifuged at 38,000 rpm for 3 h in Ti45 ultracentrifugation rotor. Membrane pellets were resuspended in 50 mM KP_i pH 7.5 using a homogenizer, flash frozen, and stored at -80 ˚C.

Western Blot Analysis

Protein samples were transferred from SDS-PAGE gels to nitrocellulose membranes for one hour at 400 mA, 100V, 30W in a transfer buffer of 194 mM glycine, 15 mM Tris base, 20% methanol. Membranes were incubated in a blocking buffer (Qiagen) for one hour while shaking, followed by an incubation in similar conditions with anti-pentahistidine horseradish peroxidase conjugate antibody solution (Qiagen) for

one hour. Membranes were washed with TBS and TBST+T (20 mM Tris-HCl pH 7.5, 1 M NaCl; + 0.2% v/v Triton X-100, 0.05% Tween 20), rinsed with water and developed in a detection solution of Pierce's SuperSignal West Pico Chemiluminescent Substrate.

Large Scale Expression

Chimeric Permeases

E. coli XL1Blue cells transformed with the appropriate plasmids were grown in 10-L BioFlo 2000 fermenters to OD_{600nm}= 0.6 in LB broth at 37 ˚C with stirring at 300 rpm. Oxygen content was varied between 5-10 L O_2/minute across separate trials. Culture was induced to 0.4 mM IPTG, temperature lowered to 32˚C and stirring to 50 rpm for 3 hrs. Induction temperature was varied between 18-37˚C across separate trials. Cells were harvested at 6800 rpm x15 min/L, resuspended and washed in 50 mM KP_i pH 7.5. Pellets were flash frozen and stored at -80 ˚C.

Double-Trp LacY Mutant

E. coli C41 cells transformed with the 2W-LacY-pT7-5 plasmid were grown in the aforementioned fermenters to OD_{600nm}= 0.6 in LB broth at 37 ˚C with stirring at 350 rpm. Culture was induced to 0.3 mM IPTG, temperature lowered to 32˚C and stirring to 50 rpm for 5 hrs. Oxygen content was maintained at 10 L O_2/minute throughout. Cells were harvested and stored as described above for the chimeric permease constructs.

Purification

Chimeric Permeases

Membranes were solubilized with 2% DDM on ice for 30 min with stirring. Membrane suspension was ultracentrifuged at 60,000 rpm for 20 min in Beckman Ti-70 rotor. Supernatants were combined and NaCl was added to 200 mM, Imidazole to 5 mM and pH adjusted to 7.6 by addition of 0.5 M dibasic NaP_i pH 10. Extract was applied to 5 mL TALON resin column equilibrated in column buffer (50 mM NaP_i pH 7.6, 0.02% DDM, 200 mM NaCl, 5 mM Imidazole) at flow rate 1-2 mL/min. Non-absorbed material was washed with column buffer, followed by wash with Buffer A (50 mM NaP_i pH 7.6, 0.02% DDM, 190 mM NaCl, 15 mM Imidazole) and elution with Buffer B (50 mM NaP_i pH 7.6, 0.02% DDM, 150 mM Imidazole). Elution volumes were concentrated in 100 molecular weight cut off (MWCO) Amicon Ultra-15 centrifugal filter units at 3500 rpm in swinging bucket rotors to a final volume of ~1 mL before dilution with Buffer C (50 mM NaP_i pH 7.6, 0.02% DDM) to 15 mL and further concentration to 5-10 mg/mL. Buffer was then exchanged to Buffer D (50 mM HEPES pH 7.6, 0.02% DDM) to remove phosphate.

Double-Trp LacY Mutant

Membranes were solubilized, NaCl (200 mM final concentation) and Imidazole (5 mM final concentration) were added, and pH was adjusted to 7.6 as described above. Extract was similarly applied to a 5 mL TALON resin column equilibrated in a column

buffer consisting of 50 mM NaP_i pH 7.6, 0.01% DDM, 200 mM NaCl, 5 mM Imidazole. Non-absorbed material was washed with this column buffer, followed by wash with Buffer C (50 mM NaP_i pH 7.6, 0.01% DDM, 190 mM NaCl, 10 mM Imidazole) to baseline. Detergent was exchanged by washing with 10 column volumes of Buffer D (50 mM NaP_i pH 7.6, 0.2% NG). Protein was eluted in ~5 column volumes elution buffer (20 mM HEPES pH 6.5, 0.2% NG, 200 mM Imidazole). Elution fractions were analyzed by SDS-PAGE and concentrated using 50 MWCO Amicon Ultra-15 centrifugal filter units at 3500 rpm in swinging bucket rotors to a final volume of ~0.4 mL and diluted to 15 mL in an imidazole-free buffer consisting of 20 mM HEPES pH 6.5, 0.2% NG. This solution was concentrated again in the same manner to ~0.5 mL and loaded onto an S-200 FPLC size exclusion chromatography column (GE Healthcare). The eluted fractions were analyzed by SDS-PAGE and concentrated to 8.6 mg/mL before crystallization.

Protein Crystallization

Chimeric Permeases

Both L6_cyt_N2C5 LacY and L6_cyt_N2C5_C154G LacY were subject to crystallization using robotic methodology at the UCLA-DOE's Crystallization Core Facility. Protein was centrifuged at 14,000 rpm for 2 minutes prior to incubation with 4-nitrophenyl α-D-galactoside (NPG) to 0.5 mM. Hanging drop vapor diffusion crystallization setups were performed with commercially available sparse matrix screens specific for membrane proteins. L6_cyt_N2C5 LacY was subjected to Molecular Dimensions Limited MemGold Screen in 96-well tray at a protein concentration of 3.8

mg/mL. L6_cyt_N2C5_C154G LacY was subject to MemGold as well as Qiagen's MbClassI and MbClass II screens at a protein concentration of 7.5 mg/mL, also in 96-well trays. Three different drop ratios (protein:reservoir, 1:1, 1:2, 2:1) were attempted in 210 nL volume drops.

Double-Trp LacY Mutant

Each protein preparation was adjusted to 8.6 mg/mL and subject to crystallization using robotic methodology at the UCLA-DOE's Crystallization Core Facility. Protein was centrifuged at 13,000 rpm for 5 minutes after incubation with octyl-β-D-galactopyranoside to 1 mM. Hanging drop vapor diffusion crystallization setups were performed with commercially available sparse matrix screens. Screens included MemGold, Qiagen's MbClass I, MbClassII and PACT, and Hampton Research's PEG/Ion and PEG/Ion II screens in 96-well trays. Three different drop ratios (protein:reservoir, 1:1, 1:2, 2:1) were attempted in 210 nL drops. In addition, homemade screens similar to the conditions used for crystallization by Kumar, *et al*., 2014 were attempted.

RESULTS AND DISCUSSION

DNA sequence of LacY hybrid plasmids received have missing amino acids in majority of the constructs

The LacY hybrid vector constructs containing single and double cytochrome$_{b562}$ inserts as well as the flavodoxin-1 inserts were sequenced to verify the published DNA

sequences (Prive *et al*., 1994; Engel *et al*., 2002). Surprisingly, out of the sixteen hybrid plasmid constructs received (Table 1), only two of them had the correct DNA sequence (Prive *et al*., 1994; Engel *et al*., 2002, Table 3A). The plasmids which had the correct DNA sequences are those that have single cytochrome$_{b562}$ insertions in loop 6, namely, L6_Cyt_N2C6 and L6_Cyt_N2C1 (Δ11-A195-H205) (Fig. 2 and Table 3).

The hybrid plasmid that had cytochrome$_{b562}$ insertion in loop 2 had deletion of the specific Ile residue (Table 3B) as compared to the published sequence (Engel *et al*., 2002). Similarly, as compared to the published sequences, the plasmid that had cytochrome$_{b562}$ insertion in loop 7 had deletion of specific Glu-Gln residues, whereas the plasmid that had cytochrome$_{b562}$ insertion in loop 10 had deletions of the Phe-Glu residues (Table 3B). We could explain these amino acid deletions based upon the molecular biology approach used to obtain the vector constructs (Engel *et al*., 2002). Our analysis revealed that the intervening DNA sequence coding the observed amino acids deleted lie between the *Xho1* and *Sac1* restriction sites introduced during the cloning strategy (Engel *et al*., 2002). Thus, during the restriction enzyme digestion step, the DNA translating to the missing amino acids in LacY would be excised.

The translated amino acid deletions were also observed in hybrid plasmids in which cytochrome$_{b562}$ was inserted in loops 1 and 6, loops 2 and 6, as well as in loops 6 and 10 of LacY. The specific translated amino acid(s) missing in loop 1 were Ile-Arg, in loop 2 was Ile and in loop 10 were Phe-Glu (Table 3C). These deletions could again be explained based upon the molecular biology approach used to obtain the vector constructs, as they lie between the the *Xho1* and *Sac1* restriction sites used for cloning

(Engel *et al*., 2002). Further, loop 6 in each of these constructs had 11 residues (A195-H205) deleted. An explanation for this could be that the parent LacY molecules used was LacY-Δ11 instead of the full-length LacY reported (Engel *et al*., 2002). Thus, these constructs had discrepancies in reported DNA sequences at two different respective sites.

The discrepancies in the reported flavodoxin-1 inserts in loops 1, 2, 5, 6, 7 and 10 of LacY were also observed. The specific translated amino acid(s) missing in loop 1 were Ile-Arg, in loop 2 was Ile, in loop 5 was Thr, in loop 7 were Glu-Gln and in loop 10 were Phe-Glu (Table 3D). Similar to the cytochrome$_{b562}$ hybrid plasmids (Table 3B and C), the deleted translated amino acids in flavodoxin-1 hybrid plasmids lie between the Xho1 and Sac1 sites introduced in the parent LacY sequence for cloning and thus would be excised during the restriction enzymes digestion step.

The reported LacY flavodoxin-1 hybrid constructs were also found to contain flavodoxin-2 insert instead of flavodoxin-1 (Table 3D). This was the most unexpected observation and could have been due to unforeseen reporting error in the previous publication (Engel *et al*., 2002). In our DNA sequence, the translated amino acid sequence clearly matched with the published flavodoxin-2 (Perna *et al*. 2001) and not with the flavodoxin-1 amino acid sequence (Osborne *et al*., 1991).

Expression and purification of L6_cyt_N2C5 and L6_cyt_N2C5_Δ11 in WT and with C154G mutation

The data presented in the previous section provides convincing explanation between the discrepancies observed in the current DNA sequences of the fourteen hybrid

LacY constructs when compared to the sequences reported previously. As a result, these plasmids have LacY insert with some of the residues missing. Thus, these fourteen plasmid constructs were deemed not suitable for further study.

The two plasmids, namely, L6_cyt_N2C5 and L6_cyt_N2_Δ11 each had the expected DNA sequence and were selected for further studies (Fig. 2). In each construct, C154G mutation was introduced to reduce the conformational flexibility (Smirnova *et al*., 2003). Level of expression of these four hybrid LacY proteins was then examined by Western blots. These data are shown in Fig. 4. All four LacY hybrid proteins with cytochrome$_{b562}$ inserted in loop 6 with Cys or Gly at position 154, and with or without deletion of 11 residues (A195-H205) appear to express at reasonable levels to proceed with large scale expression and purification. However, when large scale expression/ purification was attempted with the Δ11 constructs, adequate quantities of each protein could not be obtained for crystallization trials.

As compared to the Δ11 constructs, large-scale expression and purification of the full-length chimeric permease was successful in *E. coli* XL1Blue cells. TALON column purification profiles of L6_cyt_N2C5 and L6_cyt_N2C5_C154G are shown in Fig. 5A and 5B, respectively. SDS-PAGE analysis of each protein is shown in Fig. 5C. Both proteins appear to be homogenous for crystallization trials. However, several crystallization attempts using different conditions (see Materials and Methods) did not result in protein crystals and only yielded crystals that appeared to be comprised of DDM (Fig. 6). Based upon these observations, it might be necessary in future studies to remove excess DDM by size exclusion chromatography (SEC) prior to crystallization attempts.

Surprisingly, yield and solubility of the L6_cyt_N2C5 fusion constructs was lower than that of wild-type LacY. In addition, our results are in agreement with previous attempts at crystallization of the L6_cyt_N2C5 construct in which crystals were not obtained. Therefore, the cytochrome$_{b562}$ insertion strategy might not be useful in improving the crystallization potential of LacY.

Expression and purification of the double-Trp LacY mutant

While the aforementioned studies were in progress, the structure of the double-Trp (G46W/G262W) LacY mutant with bound TDG was determined at 3.5 Å resolution (Kumar *et al*., 2014). LacY in this structure has a partially occluded, outward-facing conformation open to the periplasmic side. Based upon this new information and in light of the unsuccessful attempts to crystallize the cytochrome$_{b562}$-LacY fusion proteins in both previous and present studies, we sought to obtain crystals of this double-Trp LacY mutant in the presence of a different galactoside ligand such as octyl β-D-galactopyranoside. Large scale expression and purification of the double-Trp LacY mutant protein was successful. TALON column purification profile of this mutant is shown in Fig. 7A and the SDS-PAGE analysis of the elution fractions is shown in Fig. 7B. The impurities observed in these fractions were removed using FPLC S-200 size exclusion chromatography. The concentrated purified protein at this stage had a single band of the expected molecular weight (Fig. 7C) and was deemed suitable for crystallization.

Crystallization was initially attempted in a range of conditions similar to those used to successfully obtain crystals of the double-Trp mutant bound to TDG (Kumar *et al*., 2014). However, the crystals with octyl β-D-galactopyranoside could not be obtained under these conditions. Thus, we proceeded to use commercial screens containing common crystallization conditions for membrane proteins. Surprisingly, of the several crystallization conditions attempted, 23 conditions listed in Table 4 yielded protein crystals. Crystals obtained under two of the conditions are shown in Fig. 8. These crystals were tested for diffraction at the Advanced Photon Source (Argonne National Laboratories), Chicago, Il. The crystals diffracted to ~20 Å (Fig. 9), indicating a need for further optimization of crystallization conditions in order to obtain better-diffracting crystals. We point out here that although crystals with TDG diffracted to a higher resolution, new conditions are needed for successful crystallization with other galactosidic substrates such as octyl β-D-galactopyranoside, which contains only one galactoside ring as opposed to the two rings present in TDG.

Strategies to obtain LacY in fully outward-open conformation

Based upon the double-Trp mutation strategy used in the recent structure determination of LacY with partially occluded outward-open conformation (Kumar *et al*., 2014), it is reasonable to propose additional mutations in residues in helix5 and helix8 surrounding the Trp46 (helix 5) and Trp262 (helix8) to obtain fully outward-open conformation in LacY. In one strategy, four additional Trp mutations in the double-Trp (G46W/G262W) are introduced (Fig. 10A). These mutations include A155W and G159W

in helix5, Q241W in helix7 and G370W in helix11. In the second strategy, four Arg mutations in the double-Trp (G46W/G262W) are introduced (Fig. 10B). These mutations include A155R and G159R in helix5, Q241R in helix7 and G370R in helix11. Note that in both strategies the same residues are either replaced with Trp or Arg. The concept behind this approach is to either increase the distance between the helices by bulky Trp residues (Fig. 10A) or by electrostatic repulsion (Fig. 10B). When mutated structures were subjected to energy minimization using CHARMM (Brooks *et al*., 2009), the resulting structures revealed further opening at the periplasmic side in the LacY double-Trp mutant (Fig. 10A and 10B). Whether these mutants would yield promising crystals and diffraction data with bound galactoside ligands remains to be determined.

Postulated conceptual configurational changes involving rotation around 1-4 thioester linkage in TDG during its transport by LacY

The crystal data presented in the two LacY structures (Abramson *et al*., 2003; Kumar *et al*., 2014) and molecular dynamics simulations (Yin *et al*., 2006; Holyoake and Sansom, 2007; Johnson and Brooker, 2009; Andersson *et al*., 2012;) were used to postulate a rotation involving the 1-4 thioester linkage during TDG transport from the periplasmic side to the cytoplasmic side. Different configurations of TDG observed in the two LacY structures (Abramson *et al*., 2003; Kumar *et al*., 2014) are shown in Fig. 11A and 11B. Although, as proposed (Guan and Kaback, 2006), the TDG in these structures is bound essentially around the same site in LacY, it shows major difference in interactions (Table 5) with the protein as well as its configuration. These two observed configurations

of TDG make the basis for the proposed mechanism of substrate transport in LacY. This is shown in Fig. 11C. In step 1, protonation of E269 breaks the hydrogen bond between E269 and W151, which, in part, contributes to the opening of the N- and C-terminal domains of LacY on the periplasmic side. In step 2, substrate enters from periplasmic side and interacts very strongly with the protein. Since concentration of substrate is limiting on the periplasmic side, the strong interaction between the substrate and the LacY are essential for binding as observed (Kumar *et al*., 2014). In step 3, the binding of the substrate triggers the translocation of the proton from E262 to E325 via H322. This results in rotation around the 1-4 thioester linkage that changes the configuration and weakens the interactions of the substrate (TDG) with LacY. Consequently, it results in a substrate-induced conformational change in LacY and closing at the periplasmic side with simultaneous opening at the cytoplasmic side. In step 4, substrate is released to the cytoplasm. Since substrate is in high concentrations on the cytoplasmic side, the weak interactions of the substrate with LacY at this stage would favor dissociation. In step 5, the release of substrate triggers the release of proton to the cytoplasm, which results in the initial ground state of LacY. One should note that the proposed mechanism is consistent with all the biochemical and crystallographic studies with the introduction of a configurational change in the substrate. Importantly, the two structures (Abramson *et al*., 2003 and Kumar *et al*., 2014) of LacY provided the needed insight for the proposed substrate configurational change during transport.

CONCLUSIONS

First, in this study, two LacY molecules with cytochrome$_{b562}$ insertions, with and without the C154G mutation were successfully expressed and crystallization was attempted. We faced difficulty in obtaining protein crystals and instead obtained crystals likely comprised of DDM. It is plausible that the cytochrome$_{b562}$ insertion is not beneficial for improving ease of handling and crystallization of LacY. Other carrier protein insertions or variable positions and linker lengths might be necessary for this approach to be fruitful. Second, we were successful in expressing and purifying the double-Trp mutant (G46W/G262W); however, our initial attempts to crystallize this protein in the presence of octyl-β-D-galactopyranoside yielded crystals which diffracted to only ~20 Å. Although the double-Trp mutant did yield diffraction-quality crystals in the presence of TDG, the presence of a different ligand could require new extensive crystallization efforts to obtain crystals of similar quality. Third, based on the recent crystal structure of LacY in an almost-occluded, open-outward conformation, we designed two mutational strategies to yield LacY molecule in a fully open, outward-facing conformation. We expect that employing these strategies will stabilize LacY in this conformation via bulky Trp residues or electrostatic repulsion by Arg residues, thereby moving the putative helices farther apart and keeping the protein in the outward-open conformation. Finally, we propose a configurational change in the substrate molecule involving a rotation around the 1,4-β linkage during transport that has not elaborated or discussed earlier.

Figure 1. Cartoon representation of LacY C154G mutant with TDG. Ribbon diagram of the LacY C154G mutant structure in fully opened inward-facing conformation adopted from Abramson *et al.* 2003. The N- and C-terminal domains of the LacY transporter are colored blue and red, respectively. The bound substrate lactose homolog, TDG, is shown in stick representation. Green represents carbon, yellow represents sulfur and red represents oxygen.

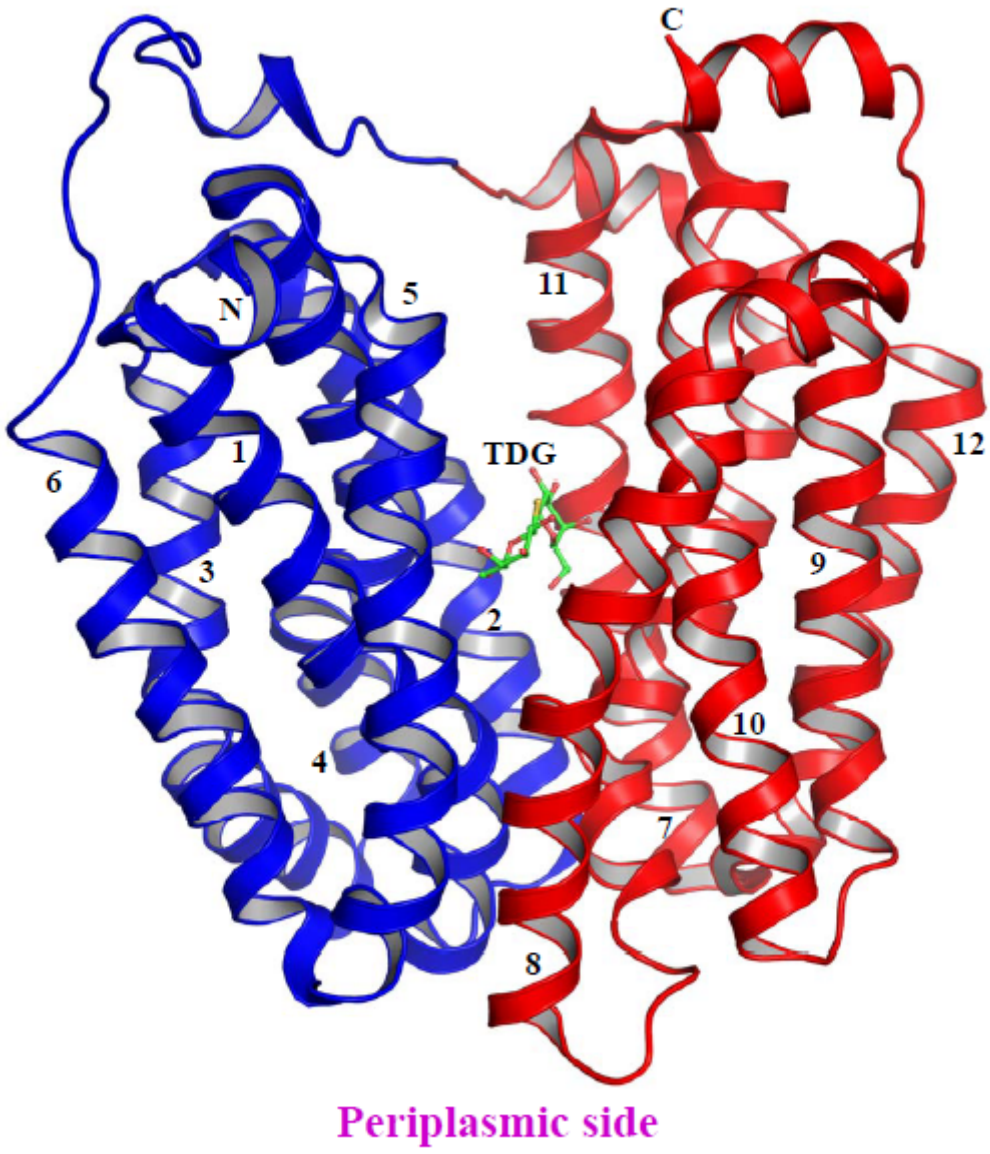
Cytoplasmic side
C
N
5
11
1
TDG
12
6
3
9
2
10
4
7
8
Periplasmic side

Figure 2. **Representative topology of the LacY delta11 (A195-H205) and cytochrome$_{b562}$-fusion chimeric permeases.** A) Schematic representation of the LacY. The sites used to insert cytochrome$_{b562}$ or flavodoxin-1 are marked with a large arrow head and the deleted residues in the L6 loop are indicated by small arrows. B) Schematic representation of the LacY with the cytochrome$_{b562}$ insert. The point mutation C154G made in the helix 5 of LacY is also marked. Loops are marked as L1, L2 etc. and the helices are marked as I, II etc. N and C represents amino and C-terminal of LacY. PL, phospholipid membrane.

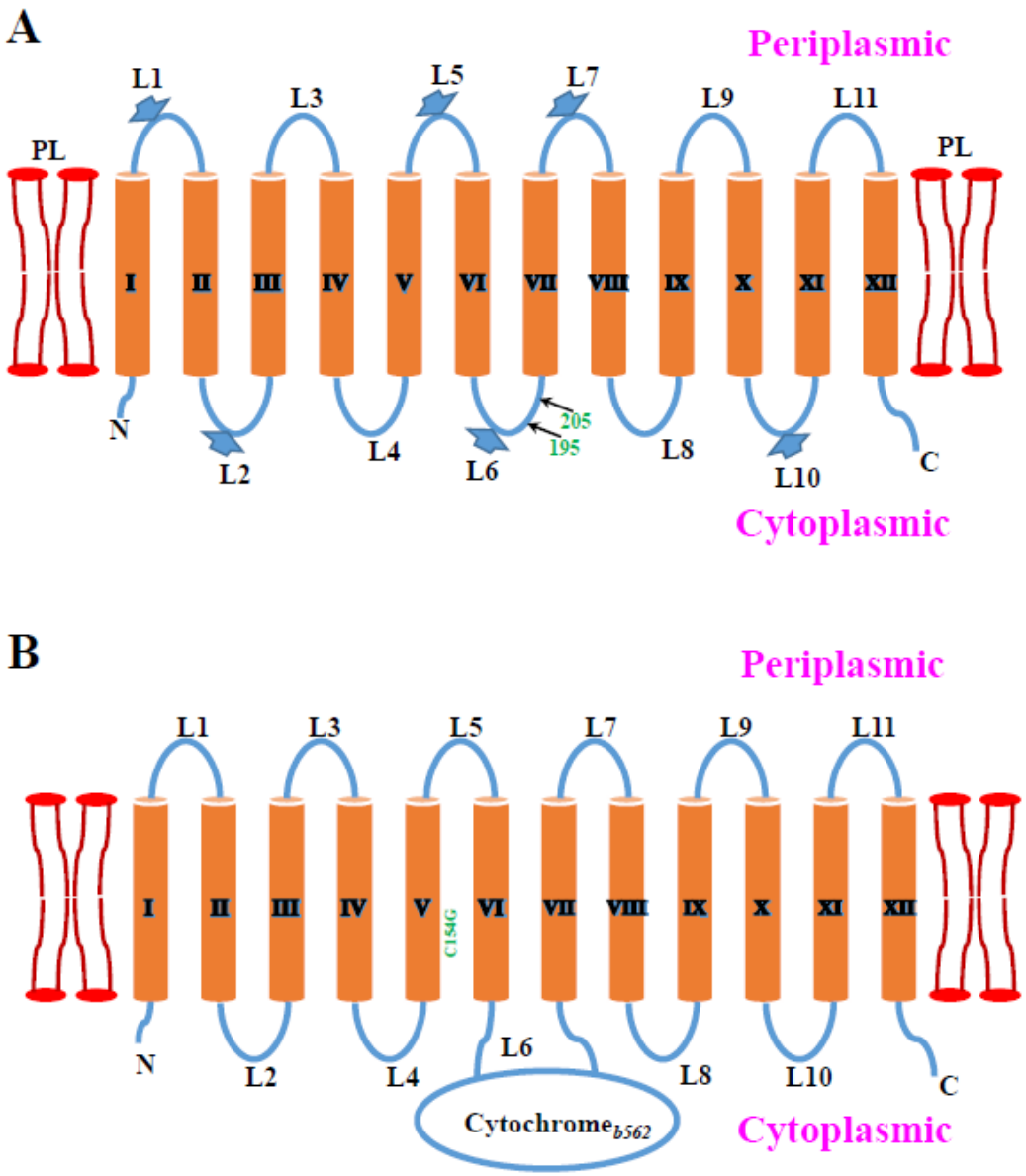
A
Periplasmic
L1
L3
L5
L7
L9
L11
PL
PL
I
II
III
IV
V
VI
VII
VIII
IX
X
XI
XII
N
L2
L4
L6
205
195
L8
L10
C
Cytoplasmic
B
Periplasmic
L1
L3
L5
L7
L9
L11
I
II
III
IV
V
C154G
VI
VII
VIII
IX
X
XI
XII
N
L2
L4
L6
L8
L10
C
Cytochrome$_{b562}$
Cytoplasmic

Table 1. List of LacY hybrid constructs selected for screening.

S. No	Plasmid
	LacY with Single cytochrome insert
1	L6_Cyt_N2C6
2	L6_Cyt_N2C1 *(Δ11*-195-205)
3	L2_Cyt_N2C1
4	L7_Cyt_N2C1
5	L10_Cyt_N2C1
	LacY with Double cytochrome insert
6	L1_Cyt/L6_Cyt
7	L2_Cyt/L6_Cyt
8	L6_Cyt/L10_Cyt
	LacY with Flavodoxin insert
9	L1_Fla_N5C5
10	L2_Fla_N1C1
11	L2_Fla_N2C5
12	L5_Fla_N5C5
13	L6_Fla_N1C1
14	L7_Fla_N5C5
15	L10_Fla_N1C1
16	L10_Fla_N1C1

Hydrophilic loop of LacY in which the carrier protein is inserted (e.g. L1 lies between helices 1 and 2). N1C1 and N2C5 refer to amino acid linker lengths between the N-terminal and C-terminal regions of the carrier protein (Engel, *et al*. 2002). Finally, the Δ11 construct contains a deletion of 11 residues (A195-H205) in the L6 cytoplasmic loop of LacY.

Figure 3. Cartoon representation of the double-Trp LacY mutant with TDG. Ribbon diagram of the LacY G46W/G262W mutant structure in partially occluded outward-facing conformation adopted from Kumar *et al.* 2014. The N- and C-terminal domains of the LacY transporter are colored blue and red, respectively. The bound substrate lactose homolog, TDG, is shown in stick representation. Green represents carbon, yellow represents sulfur and red represents oxygen. The positions of the two tryptophan residues mutated are marked.

Cytoplasmic side

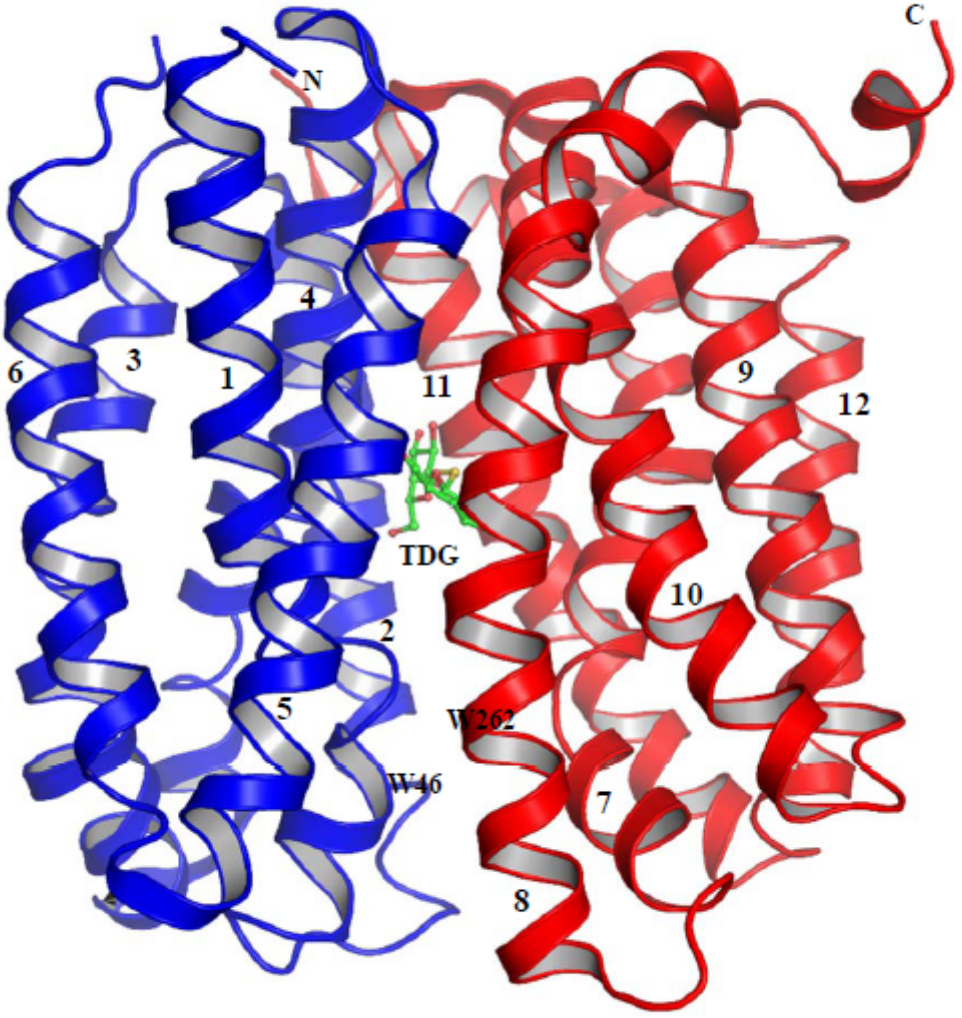

Periplasmic side

Table 2. *Escherichia coli* strains used for expression of LacY hybrid proteins.

Strain	Genotype
XL1Blue	endA1 gyrA96(nal^R) thi-1 recA1 relA1 lac glnV44 F'[::Tn10 proAB$^+$ lacI^q Δ(lacZ)M15] hsdR17(r_K^- m_K^+)
C41 (Walker)	F$^-$ *ompT hsdS*$_B$ (r_B^- m_B^-) *gal dcm* (DE3)

Table 3: Comparison between observed and published DNA sequences of LacY fusion permeases with cytochrome$_{b562}$ and flavodoxin inserts

A. Cyt$_{b562}$ insert in loop (L) 6 of LacY with and without deletion of 195-205 residues

Construct*	LacY	Linker (NH_2)	Insert (Cyt$_{b562}$)	Linker (COOH)	LacY	Sequence	Comment
L6_Cyt_N2C6	190-DAPS	SA	$_N$ADLED . . . HQKYR$_C$	SFLISS	194-SATV-197	Published[a]	Confirmed in the current study
	190-DAPS	SA	$_N$ADLED . . . HQKYR$_C$	SFLISS	194-SATV-197	Current Study	
L6_Cyt_N2C1	190-DAPS	SA	$_N$ADLED . . . HQKYR$_C$	S	S(195-205 Del)SAFS-209	Published[b]	Confirmed in the current study
Δ11-195-205	190-DAPS	SA	$_N$ADLED . . . HQKYR$_C$	S	S(195-205 Del)SAFS-209	Current Study	

* The constructs are listed in the same order as in Table 1
[a] Prive *et al*. 1994; [b] Engel *et al*. 2002

B. Cyt$_{b562}$ inserts in each of the loops L2, L7 and L10 of LacY

Construct*	LacY	Linker (NH_2)	Insert (Cyt$_{b562}$)	Linker (COOH)	LacY	Sequence	Comment
L2_Cyt_N2C1	70-LGSS[c]	SA	$_N$ADLED . . . HQKYR$_C$	S	ISSLRK-74	Published[b]	I missing in the current study
	70-LGSS	SA	$_N$ADLED . . . HQKYR$_C$	S	-SSLRK-74	Current Study	
L7_Cyt_N2C1	251-FASS[d]	SA	$_N$ADLED . . . HQKYR$_C$	S	EQSSRV-260	Published[b]	EQ missing in the current study
	251-FASS	SA	$_N$ADLED . . . HQKYR$_C$	S	--SSRV-260	Current Study	
L10_Cyt_N2C1	337-ITSS	SA	$_N$ADLED . . . HQKYR$_C$	S	FESSFS-346	Published[b]	FE missing in the current study
	337-ITSS	SA	$_N$ADLED . . . HQKYR$_C$	S	- -SSFS-346	Current Study	

*The constructs are listed in the same order as in Table 1
[b]Engel *et al*. 2002;[c] double underlines indicate insertions (Engel *et al*. 2002);[d] Single underlines indicate substitutions (Engel *et al*. 2002)

Table 3 (Continued):

C. Cyt_{b562} inserts in loops 1 and 6, loops 2 and 6, as well as in loops 6 and 10 of LacY

Construct*	LacY	Linker (NH_2)	Insert (Cyt_{b562})	Linker (COOH)	LacY	Sequence	Comment
L1_Cyt/L6_Cyt							
L1 loop	36-DISS[d]	SA	NADLED . . . HQKYRC	S	IRSSD-44	Published[b]	IR in L1 and residues 195-205 in L6 missing in the current study
	36-DISS	SA	NADLED . . . HQKYRC	S	- -SSD-44	Current Study	
L6 loop	190-DAPS	SA	NADLED . . . HQKYRC	S	194-SATV-197	Published[b]	
	190-DAPS	SA	NADLED . . . HQKYRC	S	S(195-205 Del)SAFS-209	Current Study	
L2_Cyt/L6_Cyt							
L2 loop	70LGSS[c]	SA	NADLED . . . HQKYRC	S	ISSLRK-74	Published[b]	I in L1 and residues 195-205 in L6 missing in the current study
	70LGSS	SA	NADLED . . . HQKYRC	S	-SSLRK-74	Current Study	
L6 loop	190-DAPS	SA	NADLED . . . HQKYRC	S	194-SATV-197	Published[b]	
	190-DAPS	SA	NADLED . . . HQKYRC	S	S(195-205 Del)SAFS-209	Current Study	
L6_Cyt/L10_Cyt							
L6 loop	190-DAPS	SA	NADLED . . . HQKYRC	S	194-SATV-197	Published[b]	FE in L10 and residues 195-205 in L6 missing in the current study
	190-DAPS	SA	NADLED . . . HQKYRC	S	S(195-205 Del)SAFS-209	Current Study	
L10 loop	337-ITSS	SA	NADLED . . . HQKYRC	S	FESSFS-346	Published[b]	
	337-ITSS	SA	NADLED . . . HQKYRC	S	- -SSFS-346	Current Study	

*The constructs are listed in the same order as in Table 1

[b]Engel *et al*. 2002;[c] double underlines indicate insertions (Engel *et al*. 2002);[d] Single underlines indicate substitutions (Engel *et al*. 2002)

Table 3 (Continued):

D. Reported Flavodoxin1 (Fla, PDB code 1AG9) inserts in loops 1, 2, 5, 6, 7 and 10 of LacY

Construct*	LacY	Linker (NH_2)	Insert (Flavodoxin)	Linker (COOH)	LacY	Sequence	Comment (see footnote 'e' also)
L1_Fla_N5C5	36-DISS[d]	SGGSG	$_N$MAITGI . . . ELHLD$_C$	GSGGS	IRSSD-44	Published[b]	IR missing in the current study and sequence insert conflict[e]
	36-DISS	SGGSG	$_N$MNMGL . . . EMAEH$_C$	GSGGS	--SSD-44	Current Study	
L2_Fla_N1C1	70-LGSS	S	$_N$MAITGI . . . ELHLD$_C$	S	ISSLRK-74	Published[b]	I missing in the current study and sequence insert conflict[e]
	70-LGSS	S	$_N$MNMGL . . . EMAEH$_C$	S	-SSLRK-74	Current Study	
L2_Fla_N2C5	70-LGSS[c]	SGGSG	$_N$MAITGI . . . ELHLD$_C$	GSGGS	ISSLRK-74	Published[b]	I missing in the current study and sequence insert conflict[e]
	70-LGSS	SGGSG	$_N$MNMGL . . . EMAEH$_C$	GSGGS	-SSLRK-74	Current Study	
L5_Fla_N5C5	159-GISS	SGGSG	$_N$MAITGI . . . ELHLD$_C$	GSGGS	TSSNQ-167	Published[b]	T missing in the current study and sequence insert conflict[e]
	159-GISS	SGGSG	$_N$MNMGL . . . EMAEH$_C$	GSGGS	-SSNQ-167	Current Study	
L6_Fla_N1C1	190-DAPS	S	$_N$MAITGI . . . ELHLD$_C$	S	SATV-197	Published[b]	No missing residues but sequence insert conflict[e]
	190-DAPS	S	$_N$MNMGL . . . EMAEH$_C$	S	SATV-197	Current Study	
L7_Fla_N5C5	251-FASS	SGGSG	$_N$MAITGI . . . ELHLD$_C$	GSGGS	EQSSRV-260	Published[b]	EQ missing in the current study and sequence insert conflict[e]
	251-FASS	SGGSG	$_N$MNMGL . . . EMAEH$_C$	GSGGS	--SSRV-260	Current Study	
L10_Fla_N1C1	337-ITSS	S	$_N$MAITGI . . . ELHLD$_C$	S	FESSFS-346	Published[b]	FE missing in the current study and sequence insert conflict[e]
	337-ITSS	S	$_N$MNMGL . . . EMAEH$_C$	S	- -SSFS-346	Current Study	
L10_Fla_N1C1	337-ITSS	SGGSG	$_N$MAITGI . . . ELHLD$_C$	GSGGS	FESSFS-346	Published[b]	FE missing in the current study and sequence insert conflict[e]
	337-ITSS	SGGSG	$_N$MNMGL . . . EMAEH$_C$	GSGGS	- -SSFS-346	Current Study	

*The constructs are listed in the same order as in Table 1

[b]Engel *et al*. 2002;[c] double underlines indicate insertions (Engel *et al.* 2002);[d] Single underlines indicate substitutions (Engel *et al*. 2002)

[e] Reported Fla insert is of *E. coli* flavodoxin-1 (Osborne *et al.* 1991); however, the current sequence in each construct reveals that the insert is of *E. coli* flavodoxin2 (Perna *et al*. 2001) and not of flavodoxin-1.

Figure 4. Western blots of expression of LacY cytochrome-fusion proteins (L6_cyt_N2C5 and L6_cyt_N2C5_Δ11) in WT and C154G mutant. *E. Coli* XL1Blue cells transformed with the appropriate plasmids were grown in LB broth in 25 mL cultures. Expression of the protein was induced with 0.4 mM IPTG for 4 hrs. Cells were lysed and the membranes were isolated as detailed in "Materials and Methods". The membranes prepared from cells transformed with plasmid without the insert served as a negative control and the membranes prepared from the cells with wild-type LacY served as a positive control. Relative expression of each protein was assessed by Western blots as outlined in Materials and Methods section. Ten μg of total membrane proteins was loaded in each lane. Lane 1, MW markers; lane 2, wild-type LacY; lane 3, PT7-5 vector without the insert; lane 4, L6_cyt_N2C5_Δ11; lane 5, L6_cyt_N2C5; lane 6, L6_cyt_N2C5_Δ11 with C154G mutation; and lane 7, L6_cyt_N2C5 with C154G mutation.

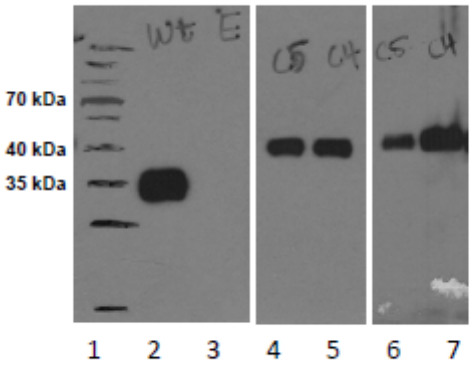
70 kDa
40 kDa
35 kDa
Wt
E
C5
C4
C5
C4
1
2
3
4
5
6
7

Figure 5. Expression and purification of the LacY cytochrome-fusion proteins (L6_cyt_N2C5) in WT and C154G mutant. Elution profile for TALON column purification of the L6_cyt_N2C5 construct without (A) and with C154G (B) mutation. Arrow 1 indicates the addition of buffer A (50 mM NaP_i pH 7.6, 0.02% DDM, 190 mM NaCl, 15 mM imidazole) and arrow 2 indicates the elution step with buffer B (50 mM NaP_i pH 7.6, 0.02% DDM, 150 mM imidazole). C) SDS-PAGE gel analysis of the purified proteins. Lane 1, MW markers; lane 2, L6_cyt_N2C5; lane 3, L6_cyt_N2C5_C154G.

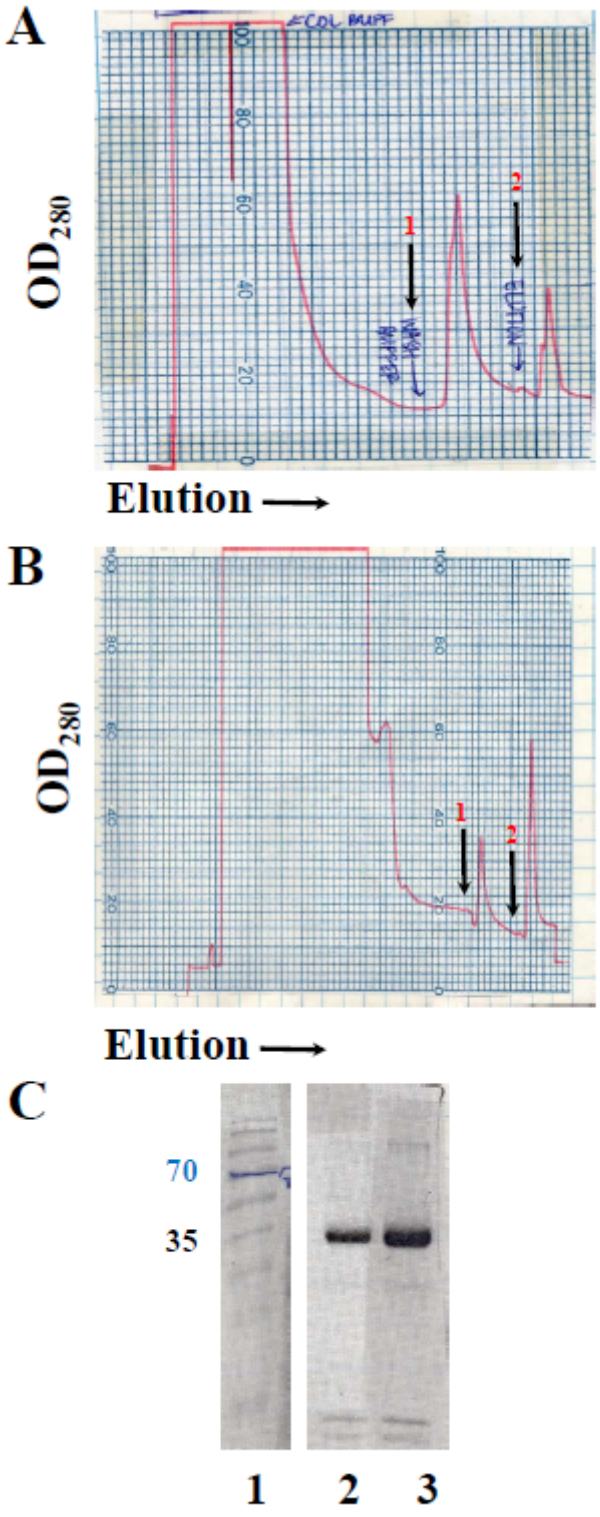
A
ECOL BUFF
100
80
60
40
20
0
1
2
OD280
Elution
B
1
2
OD280
Elution
C
70
35
1
2
3

Figure 6. Crystalline precipitate observed during L6_cyt_N2C5_C154G crystallization. Crystallization trials were performed at a protein concentration of 7.5 mg/mL with 0.5 mm 4-nitrophenyl α-D-galactoside (NPG) ligand. Shown here is the crystalline precipitate observed in Qiagen Mb Class I screen, condition 46 (0.02 M sodium citrate, 0.1 M sodium dihydrogen phosphate pH 6.2, 15% PEG 2000). Crystals appear to be comprised of DDM, as excess detergent was not removed from the protein sample prior to crystallization.

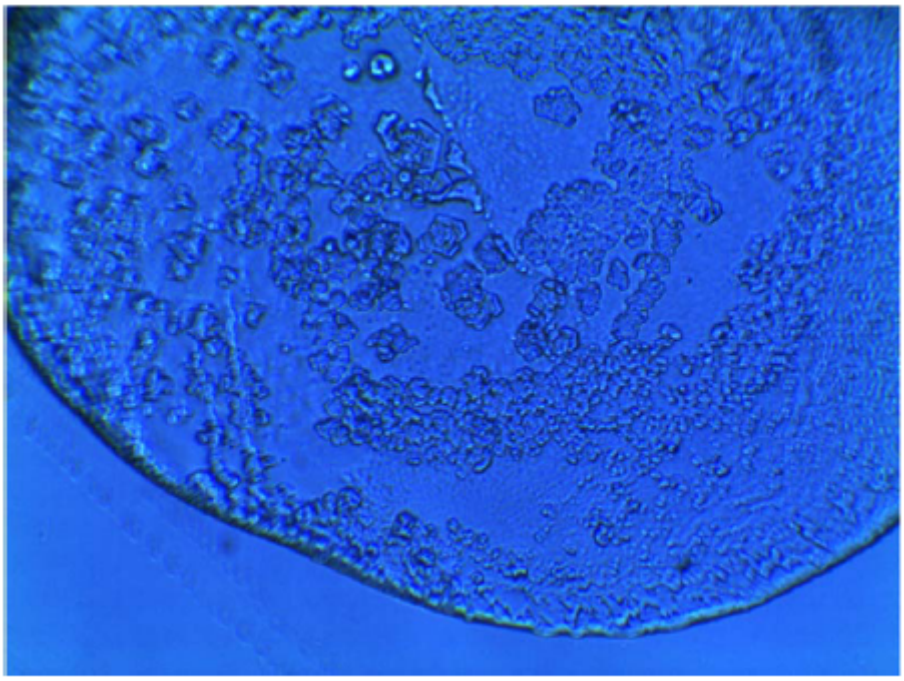

10x

Figure 7. Purification of the LacY double-Trp (G46W/G262W) mutant. A) Elution profile of the TALON column purification of the double-Trp LacY mutant. Arrow 1 indicates the addition of buffer C (50 mM NaPi, pH 7.6, 0.01% DDM, 190 mM NaCl, 10 mM imidazole), arrow 2 indicates the detergent exchange step, addition of buffer D (20 mM HEPES pH 7.6, 0.2% NG), and arrow 3 indicates the elution step with 20 mM HEPES pH 6.5, 0.2% NG, 200 mM imidazole. B) SDS-PAGE analysis of the elution fractions (200 mM imidazole) from the TALON column. The first four 5-mL elution fractions contained the target protein; 15 μL aliquot of each eluted fraction was loaded on the gel. C) SDS-PAGE analysis of the concentrated double-Trp LacY mutant after FPLC S-200 size exclusion chromatography. Eluted fractions were pooled and concentrated to 8.6 mg/mL; 1 μL of the purified sample was loaded on the gel. The left lanes in (B) and (C) depict the molecular weight standards.

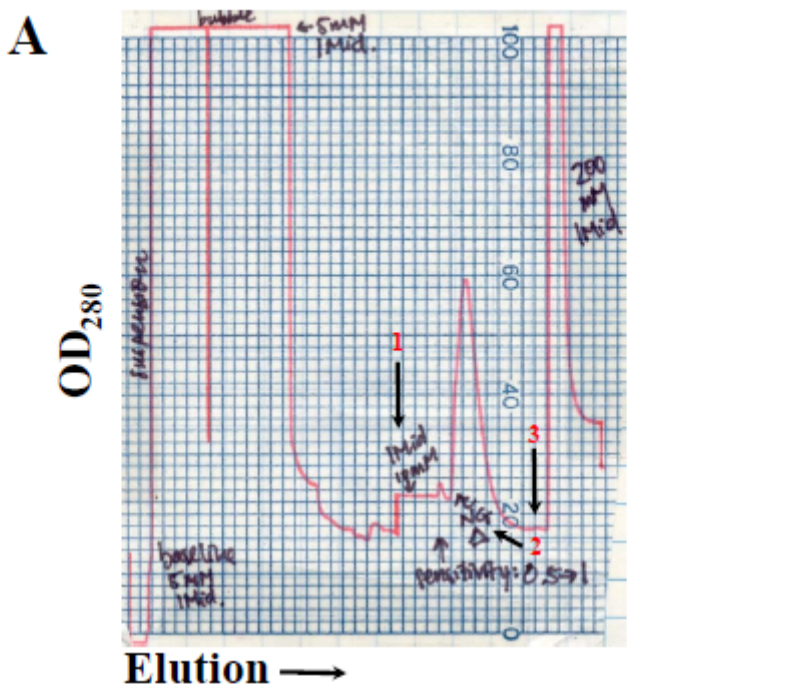
A
OD280
Elution
100
80
60
40
20
0
1
2
3
B
70 kDa
55 kDa
35 kDa
C
70 kDa
55 kDa
35 kDa

Table 4. Conditions that yielded crystals of LacY double-Trp mutant with octyl β-D galactopyranoside.

Crystal Screen	Condition Number	Chemical compositions
Molecular Dimensions MemGold™	1	0.08 M sodium citrate pH 5.2 2.2 M ammonium sulfate
Molecular Dimensions MemGold™	7	0.1 M ammonium sulfate 0.1 M HEPES pH 7.5 12.0% w/v polyethylene glycol (PEG) 4000 22% v/v glycerol
Molecular Dimensions MemGold™	11	0.15 M potassium phosphate pH 6.5 3.3 M ammonium sulfate
Molecular Dimensions MemGold™	13	0.1 M sodium chloride 0.02 M sodium citrate pH 5.6 11% w/v PEG 3350
Molecular Dimensions MemGold™	18	0.2 M sodium chloride 0.025 M HEPES pH 7.5 13% w/v PEG 400
Molecular Dimensions MemGold™	19	0.1 M HEPES pH 7.5 11% w/v PEG 3350
Molecular Dimensions MemGold™	37	0.2 M calcium chloride 0.1 M HEPES pH 7.5 53% v/v PEG 400
Molecular Dimensions MemGold™	38	0.05 M magnesium acetate 0.05 M sodium acetate pH 5.0 28% v/v PEG 400
Molecular Dimensions MemGold™	41	0.05 M magnesium acetate 0.05 M sodium acetate pH 5.4 24% v/v PEG 400
Molecular Dimensions MemGold™	57	0.1 M sodium chloride 0.1 M cadmium chloride 0.1 M Tris HCl pH 8.0 33% v/v PEG 400

Table 4 (Continued)

Molecular Dimensions MemGold™	58	0.1 M Bicine pH 8.9 31% w/v PEG 2000
Molecular Dimensions MemGold™	69	0.2 M calcium chloride 0.1 M HEPES pH 7.0 33% v/v PEG 400
Molecular Dimensions MemGold™	81	0.05 M sodium chloride 0.1 M sodium citrate pH 5.5 26% v/v PEG 400
Molecular Dimensions MemGold™	91	0.2 M calcium chloride 0.1 M MES pH 6.5 33% v/v PEG 400
Molecular Dimensions MemGold™	96	0.1 M BIS-TRIS propane pH 7.0 3.0 M sodium chloride
Hampton PEG/Ion	33	0.2 M sodium sulfate decahydrate pH 6.7 20 % w/v PEG 3350
Hampton PEG/Ion	39	0.2 M sodium phosphate monobasic monohydrate pH 4.7 20% w/v PEG 3350
Hampton PEG/Ion II	13	4% Tacsimate pH 6.0 12% w/v PEG 3350
Hampton PEG/Ion II	23	0.1 M DL-Malic acid pH 7.0 12% PEG 3350
Hampton PEG/Ion II	38	0.05 M citric acid, 0.04 M BIS-TRIS propane pH 5.0 16% w/v PEG 3350
Hampton PEG/Ion II	39	0.04 M citric acid, 0.06 M BIS-TRIS propane pH 6.4 20% w/v PEG 3350
Hampton PEG/Ion II	42	0.02 M calcium chloride dihydrate 0.02 M cadmium chloride hydrate 0.02 M cobalt (II) chloride hexahydrate 20% w/v PEG 3350
Qiagen MbClass II	40	0.1 M sodium chloride 0.1 M tri-sodium citrate pH 5.6 30% v/v PEG 400

Figure 8. Crystals of LacY double-Trp mutant with octyl β-D-galactopyranoside. Shown are the light (left) and UV (right) images (10x magnification) of the crystals obtained in MbClass II condition #40 (Table 4, 0.1 M sodium chloride, 0.1 M tri-sodium citrate pH 5.6, 30% v/v PEG 400) (A) and in MemGold condition #81 (Table 4, 0.05 M sodium chloride, 0.1 M sodium citrate pH 5.5, 26% v/v PEG 400) (B).

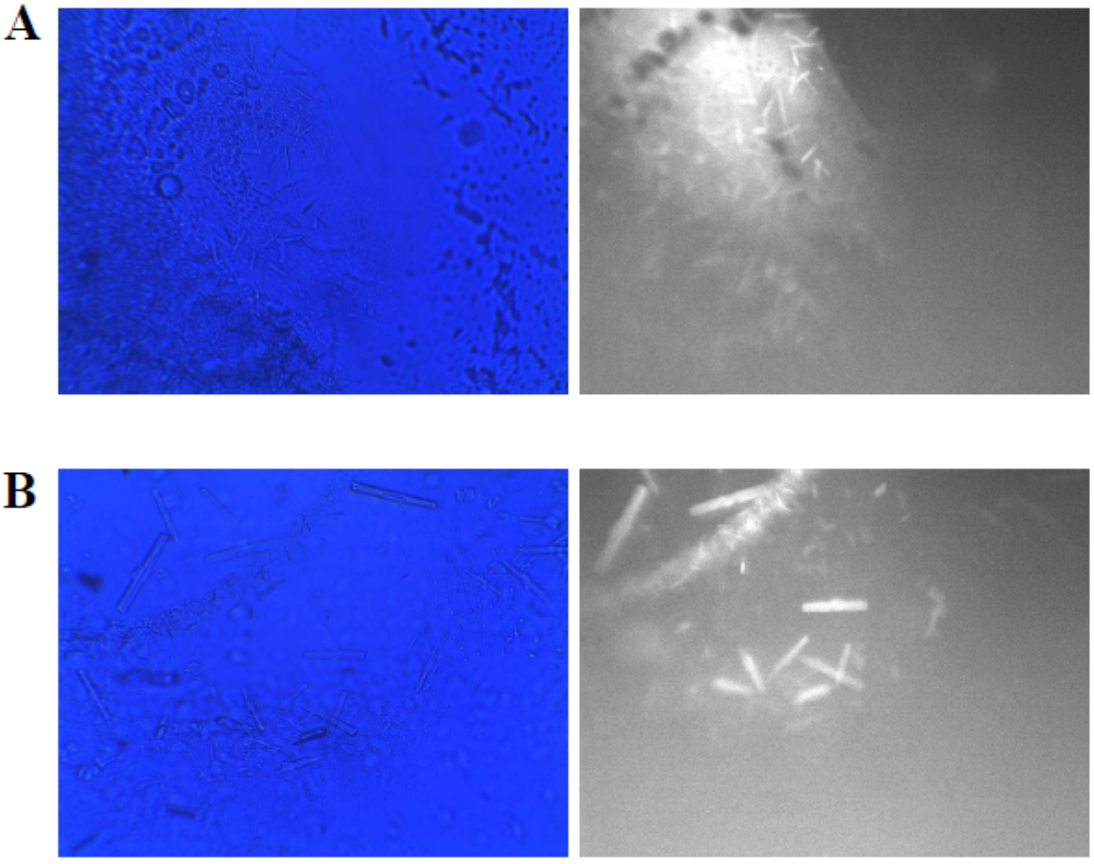
A
B

Figure 9. Diffraction pattern of LacY double-Trp mutant. Crystals were flash-frozen in liquid nitrogen and data were collected at Advanced Photon Source (Argonne National Laboratory) using beamline 24-ID-E and wavelength of .94 Å. Diffraction image was obtained from crystals obtained in Fig. 8B.

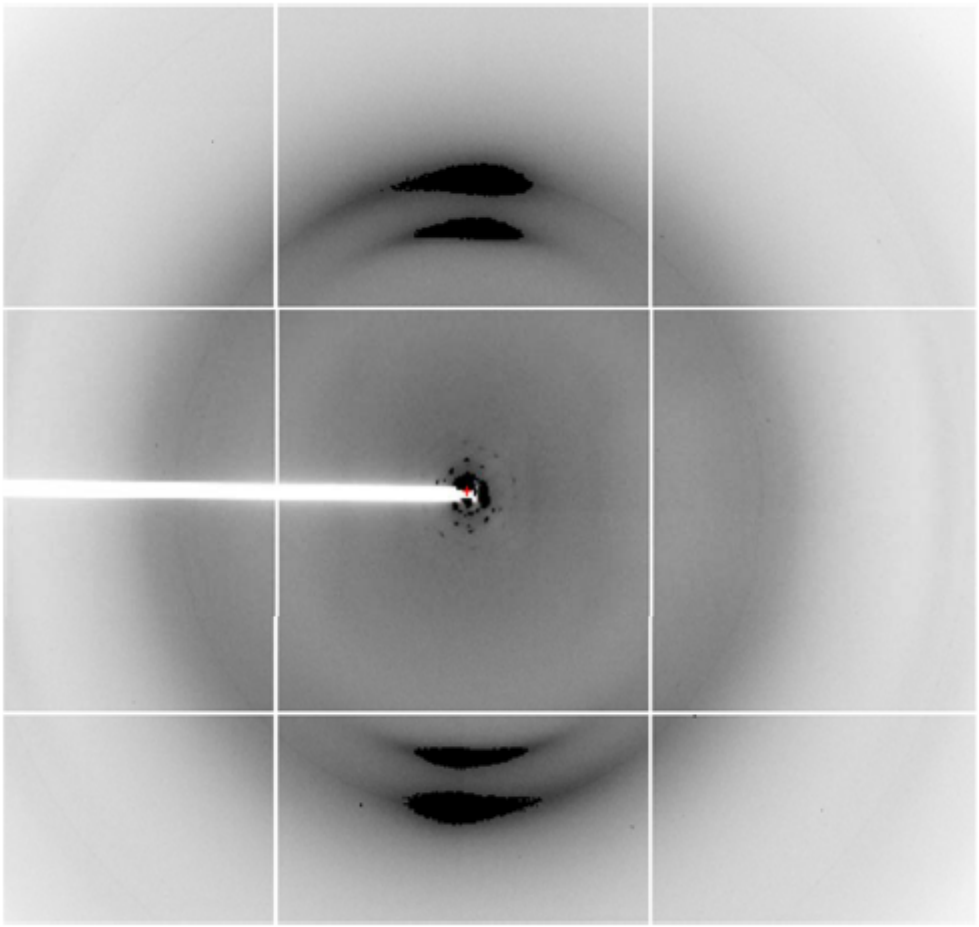

Figure 10. The proposed modeled structures of LacY with specific Trp or Arg mutations to obtain the structure in open outward-facing conformation. Both structural models were built using PDB ID 4OAA as the starting model. The residues were mutated using Pymol (Schrodinger Inc., 2013) in LacY structure and subjected to minimization using CHARMM (Brooks et al. 2009). The view on the right is obtained by rotating the structure on the left by 90° about the axis shown. The N- and C-terminal domains of the LacY transporter are colored blue and red, respectively. A. Ribbon diagrams of the LacY with Trp mutations at positions 46, 155, 159, 241, 262 and 370. B. Ribbon diagrams of the LacY with Trp mutations at positions 46 and 262 as well as Arg mutations at positions 155, 159, 241 and 370. Helices containing the above residues are depicted as h5 and h8.

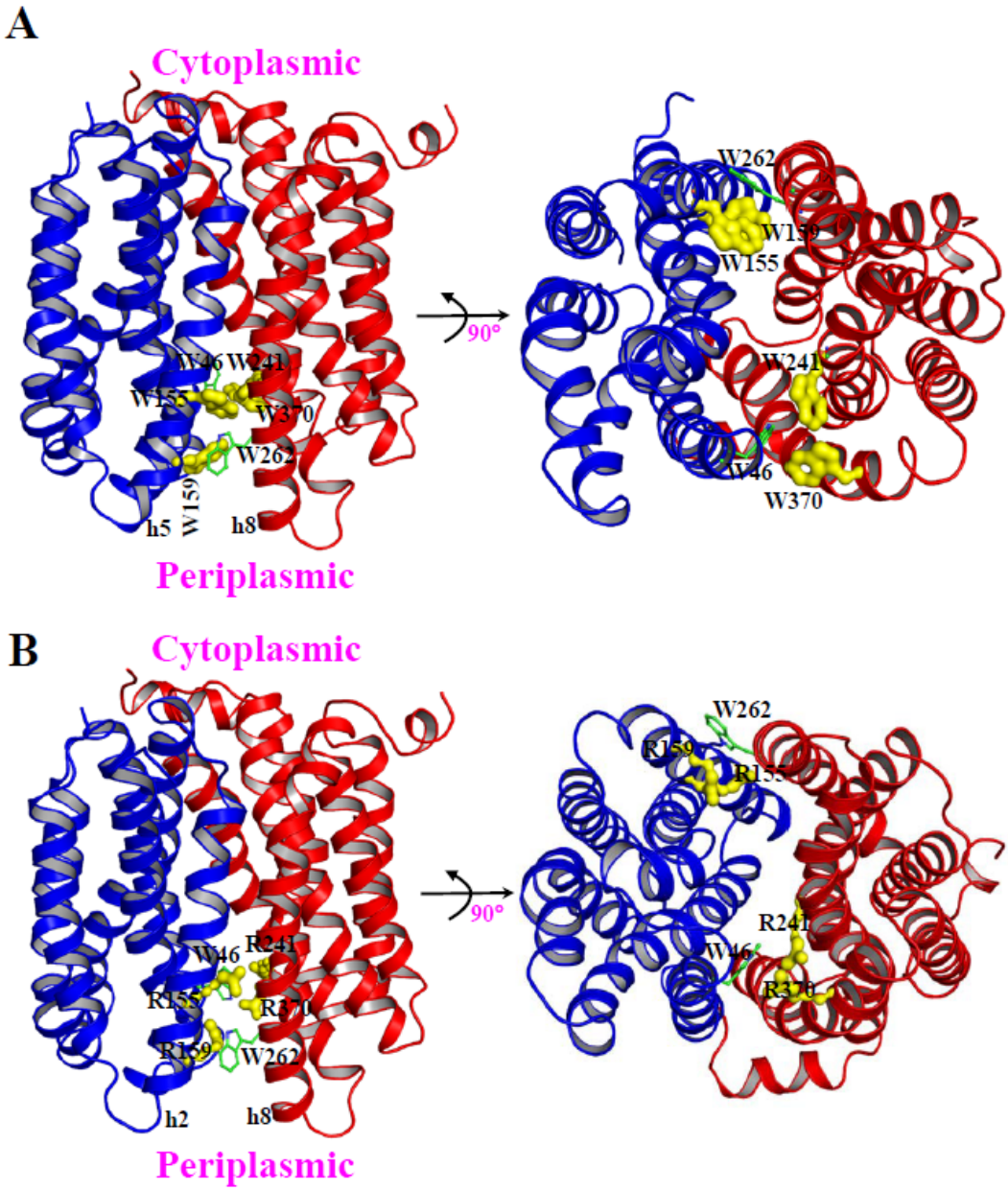
A
Cytoplasmic
W46
W241
W155
W370
W262
W159
h5
h8
90°
W262
W155
W241
W46
W370
Periplasmic
B
Cytoplasmic
W46
R241
R155
R370
R159
W262
h2
h8
90°
W262
R241
W46
R370
Periplasmic

Figure 11. Postulated conceptual configurational changes involving rotation around 1-4 thioester linkage in TDG during its transport by LacY. In A and B, the observed substrate binding modes in the two alternative conformations of LacY are shown. Ribbon diagrams of the overall structure of LacY with TDG is shown on the left. The detailed interactions between TDG and LacY are shown in the expanded view on the right and listed in Table 5. Color code for atoms: green, carbon in TDG; white, carbon in LacY; blue, nitrogen; red, oxygen; yellow, sulfur. The residues from LacY involved in substrate binding and C6, O6, C6′ and O6′ atoms in TDG are labeled. The observed hydrogen bonds and salt bridges are shown in dashed gray lines. A, The substrate TDG interaction with LacY (C154G) in the open inward-facing conformation (PDB ID 1PV7). B, TDG interaction with LacY (G46W/G262W) in the partially open outward-facing conformation (PDB ID 4OAA). C, The mechanism of TDG/H^+ co-transport outlined in five intermediate steps consistent with the crystallographic and molecular dynamics simulation data (see text for details). Partially occluded outward LacY conformation on the periplasmic side (PDB ID 4OAA) and inward-open LacY conformation on the cytoplasmic side (PDB ID 1PV7) were used as guides. Only the key residues implicated in proton transfer and substrate binding are depicted. Initially in ground state, E269 in LacY is unprotonated and is hydrogen bonded to W151. *Step 1*, Protonation of LacY. The binding of H^+ to E269 disrupts the hydrogen bond with W151 and, in part, contributes to the development of outward-open conformation in LacY. *Step 2*, Intake of TDG (or lactose) in LacY from the periplasmic side. Extensive salt bridge and hydrogen bonding

interactions between LacY residues E126, R144, E269, N172, H322 and TDG are observed (PDB ID 4OAA). *Step 3,* Proton translocation from E269 to E325. The H^+ translocation from E269 to E325 via H322 induces the configurational changes in TDG involving rotation around the 1-4 thioester linkage (shown by curved arrow); as a result this weakens the interaction between LacY and TDG and might, in part, associated with the transformation of LacY from outward-open to inward-open conformation. *Step 4*, Release of TDG to the cytoplasm. The diminished interactions between the TDG and LacY facilitate release of TDG to the cytoplasm. *Step 5,* Release of proton to the cytoplasm. In the final step, the release of H^+ from E325 to the cytoplasm induces conformational change in LacY resulting in the initial ground state.

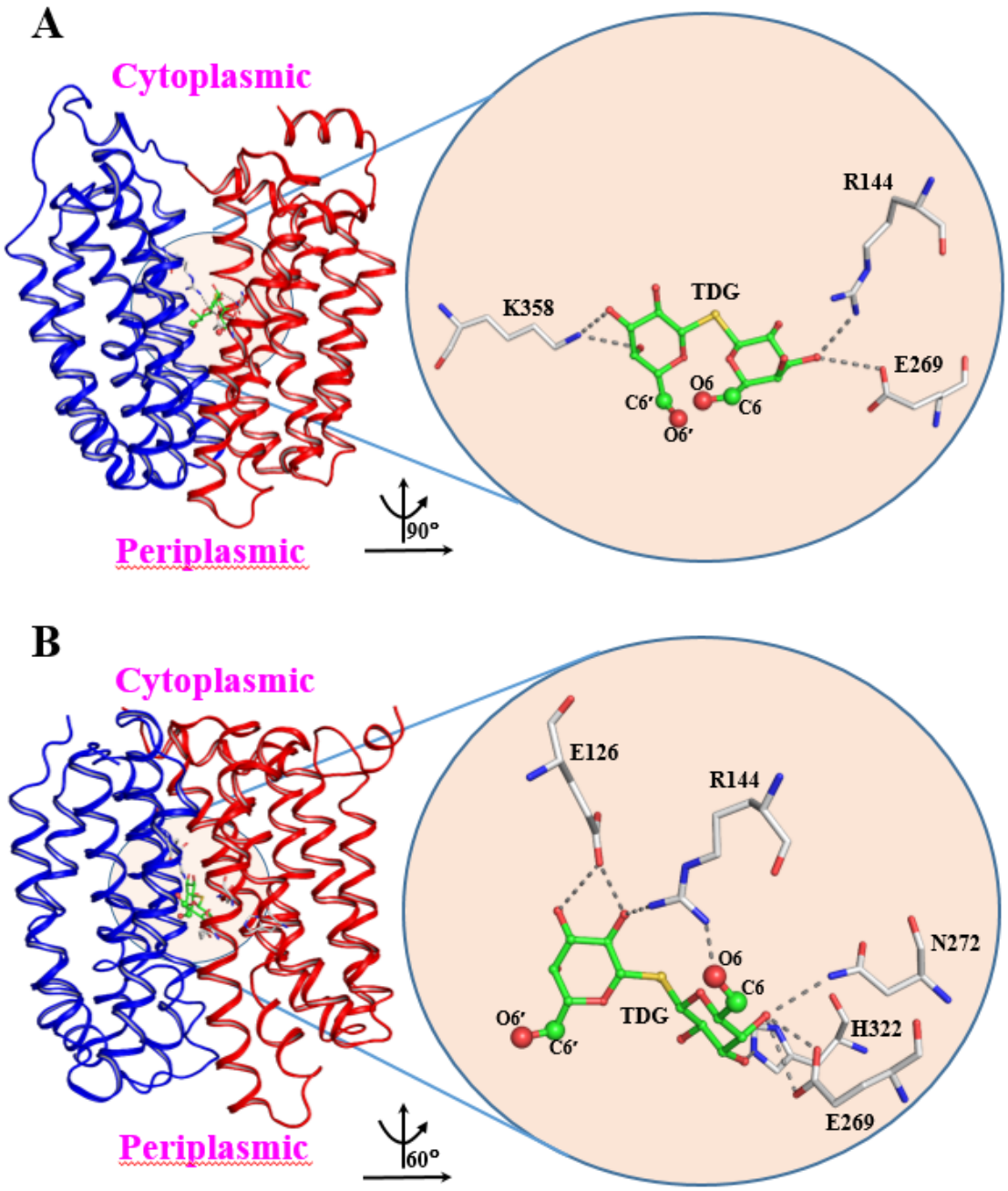
A
Cytoplasmic
Periplasmic
90°
R144
K358
TDG
E269
O6
C6
C6′
O6′
B
Cytoplasmic
Periplasmic
60°
E126
R144
N272
O6
C6
TDG
O6′
C6′
H322
E269

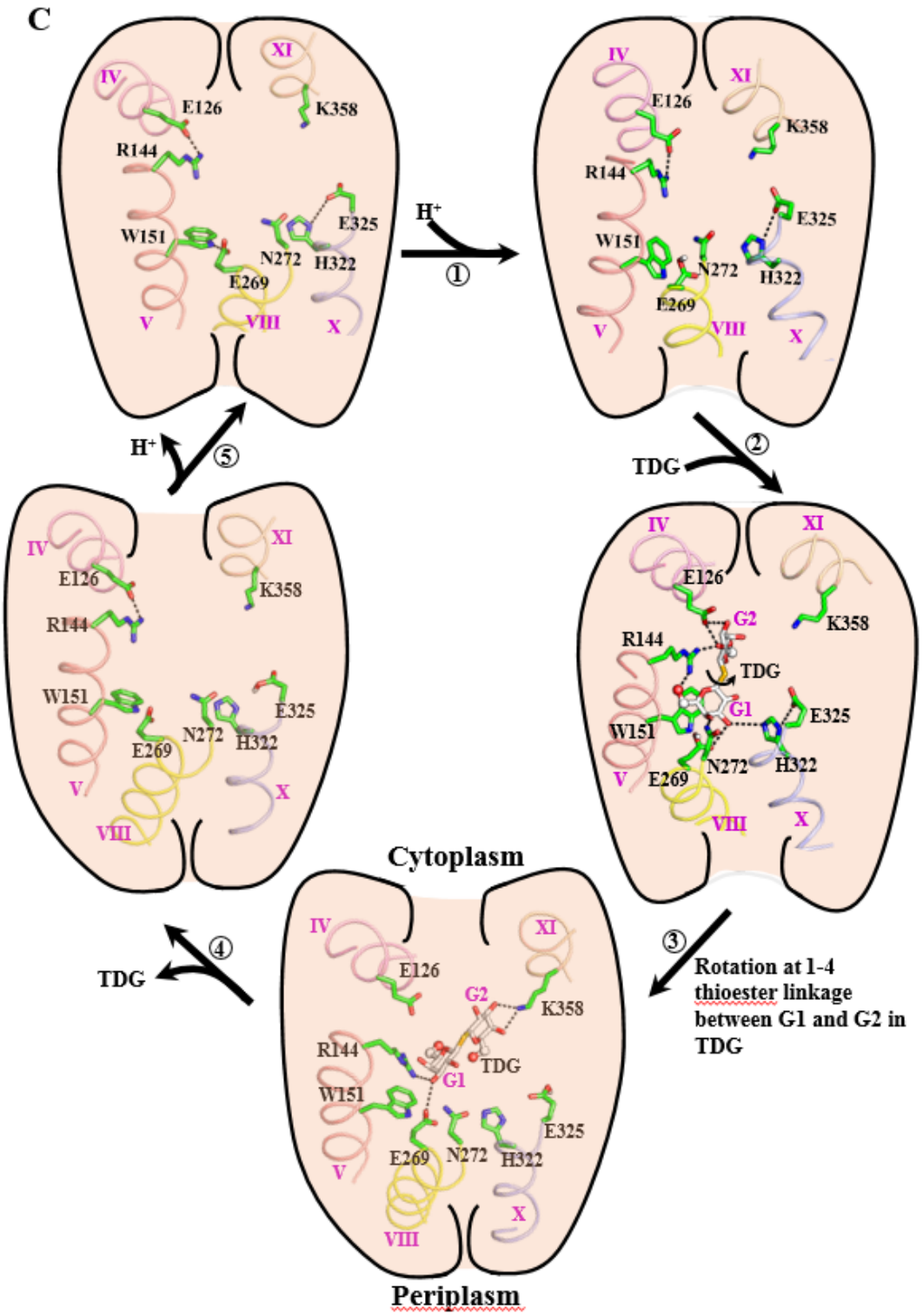
C
IV
XI
E126
K358
R144
W151
E325
N272
H322
E269
V
VIII
X
H+
①
②
TDG
③
Rotation at 1-4 thioester linkage between G1 and G2 in TDG
④
TDG
⑤
H+
G2
G1
TDG
Cytoplasm
Periplasm

Table 5. The amino acid residues involved in the interactions with TDG in inward-facing and partially occluded outward-open conformation of LacY.

LacY	TDG	Distance (Å)
Interactions observed in partially occluded outward open conformation (PDB ID, 4OAA)*		
E126:OE2	O2′	2.6
E126:OE2	O3′	3.4
R144:NH2	O2′	2.5
R144:NH1	O6	2.5
E269:OE1	O4	2.7
E269:OE2	O4	3.4
H322:NE2	O3	3.5
N272:ND2	O4	3.1
Interactions observed in inward-open conformation (PDB ID 1PV7)*		
E126:OE1	O3	3.5
R144:NH2	O3	3.1
K258:NZ	O3′	2.9

*These residues are depicted in Figure 11A and 11B.

REFERENCES

Abramson J, Smirnova I, Kasho V, Verner G, Kaback HR, Iwata S (2003) Structure and mechanism of the lactose permease of Escherichia coli. Science 301:610-615.

Andersson M, Bondar AN, Freites JA, Tobias DJ, Kaback HR and White SH. Proton-coupled dynamics in lactose permease. Structure **20**:1893-1904. 2012.

Baldwin SA. Mammalian passive glucose transporters: members of a ubiquitous family of active and passive transport proteins. Biochim Biophys Acta **1154**:17–49. 1993.

Brooks BR, Brooks CL 3rd, Mackerell AD Jr, Nilsson L, Petrella RJ, Roux B, Won Y, Archontis G, Bartels C, Boresch S, Caflisch A, Caves L, Cui Q, Dinner AR, Feig M, Fischer S, Gao J, Hodoscek M, Im W, Kuczera K, Lazaridis T, Ma J, Ovchinnikov V, Paci E, Pastor RW, Post CB, Pu JZ, Schaefer M, Tidor B, Venable RM, Woodcock HL, Wu X, Yang W, York DM and Karplus M.

CHARMM: the biomolecular simulation program. J Comput Chem. **30**:1545-1614. 2009.

Calamia J and Manoil C. Lac permease of *Escherichia coli*: topology and sequence elements promoting membrane insertion. Proc Natl Acad Sci USA **87**:4937–4941. 1990.

Chaptal V, Kwon S, Sawaya MR, Guan L, Kaback HR and Abramson J. Crystal structure of lactose permease in complex with an affinity inactivator yields unique insight into sugar recognition. Proc Natl Acad Sci USA **108**:9361-9366. 2011.

Dang S, Sun L, Huang Y, Lu F, Liu Y, Gong H, Wang J and Yan N. Structure of a fucose transporter in an outward-open conformation. Nature. **467**:734-738. 2010.

Dean M and Allikmets R. Complete characterization of the human ABC gene family. J Bioenerg Biomembr 33:475-479. 2001.

Dean M and Allikmets R. Evolution of ATP-binding cassette transporter genes. Curr Opin Genet Dev **5**:779–785. 1995.

Dean M, Rzhetsky A and Allikmets R. The human ATP-binding cassette (ABC) transporter superfamily. Genome Res 11:1156-1166. 2001.

Engel CK, Chen L and Prive GG. Insertion of carrier proteins into hydrophilic loops of the Escherichia coli lactose permease. Biochimia et Biophysicia Acta **1564**: 8-46. 2002.

Fath MJ and Kolter R. ABC transporters: bacterial exporters. Microbiol Rev 57:995–1017. 1993.

Foster DL, Boublik M and Kaback HR. J Biol Chem **258**:31- 1983.

Goswitz VC and Brooker RJ. Structural features of the uniporter/symporter/anti-porter superfamily. Protein Sci **4**:534–537. 1995.

Griffith JK, Baker ME, Rouch DA, Page MGP, Skurray RA, Paulsen IT, Chater KF, Baldwin SA and Henderson PJF. Membrane transport proteins: implications of sequence comparisons. Curr Opin Cell Biol. **4**:684–695. 1992.

Guan L and Kaback HR. Lessons from lactose permease. Annu Rev Biophys Biomol Struct 35:67-91. 2006.

Guan L, Mirza O, Verner G, Iwata S and Kaback HR. Structural determination of wild-type lactose permease. Proc Natl Acad Sci USA **104**:15294-15298. 2007.

Higgins CF. ABC transporters: from microorganisms to man. Annu Rev Cell Biol **8**:67–113. 1992.

Higgins CF. ABC transporters: physiology, structure and mechanism—an overview. Res Microbiol 152:205-210. 2001.

Holyoake J and Sansom MS. Conformational change in an MFS protein: MD simulations of LacY. Structure **15**:873-884. 2007.

Hvorup RN and Saier MH, Jr. Sequence similarity between the channel-forming domains of voltage-gated ion channel proteins and the C-terminal domains of secondary carriers of the major facilitator superfamily. Microbiology **148**:3760–3762. 2002.

Island MD and Kadner RJ. Interplay between the membrane-associated UhpB and UhpC regulatory proteins. J Bacteriol **175**:5028–5034. 1993.
Jiang X, Driessen AJ, Feringa BL and Kaback HR. The periplasmic cavity of LacY mutant Cys154→Gly: how open is open? Biochemistry. **52**:6568-6574. 2013.

Johnson JL and Brooker RJ. A K319N/E325Q double mutant of the lactose permease cotransports H^+ with lactose. Implications for a proposed mechanism of H+/lactose symport. J Biol Chem **274**:4074-4081. 2009.

Kumar H, Kasho V, Smirnova I, Finer-Moore JS, Kaback HR and Stroud RM. Structure of sugar-bound LacY. Proc Natl Acad Sci USA **111**:1784-1788. 2014.

Madej MG and Kaback HR. Evolutionary mix-and-match with MFS transporters II. Proc Natl Acad Sci U S A 110:E4831-E4838. 2013.

Madej MG and Kaback HR. The life and times of Lac permease: Crystals ain't enough. Membrane Transporter Function: To Structure and Beyond, eds Ziegler C, Kraemer R (Springer Series in Biophysics: Transporters) 2014. *in press*.

Madej MG, Dang S, Yan N and Kaback HR. Evolutionary mix-and-match with MFS transporters. Proc Natl Acad Sci U S A 110:5870-5874. 2013.

Osborne C, Chen L-M and Matthews RG. Isolation, cloning, mapping, and nucleotide sequencing of the gene encoding flavodoxin in Escherichia coli. J Bacteriol **173**:1729-1737. 1991.

Pao SS, Paulsen IT and Saier MH Jr. Major facilitator superfamily. Microbiol Mol Biol Rev **62**:1-34. 1998.

Paulsen IT, Beness AM and Saier MH., Jr. Computer-based analyses of the protein constituents of transport systems catalyzing export of complex carbohydrates in bacteria. Microbiology **143**:2685–2699. 1997.

Paulsen IT, Sliwinski MK and Saier MH Jr. Microbial genome analyses: global comparisons of transport capabilities based on phylogenies, bioenergetics and substrate specificities. J Mol Biol **277**:573-92. 1998.

Perna NT, Plunkett G 3rd, Burland V, Mau B, Glasner JD, Rose DJ, Mayhew GF, Evans PS, Gregor J, Kirkpatrick HA, Pósfai G, Hackett J, Klink S, Boutin A, Shao Y, Miller L, Grotbeck EJ, Davis NW, Lim A, Dimalanta ET, Potamousis KD, Apodaca J, Anantharaman TS, Lin J, Yen G, Schwartz DC, Welch RA and Blattner FR. Genome sequence of enterohaemorrhagic Escherichia coli O157:H7. Nature. **409**:529-533. 2001.

Privé GG, Verner GE, Weitzman C, Zen KH, Eisenberg D, Kaback HR. Fusion proteins as tools for crystallization: the lactose permease from Escherichia coli. Acta Crystallogr D Biol Crystallogr **50**:375-379. 1994.

Radestock S and Forrest LR. The alternating-access mechanism of MFS transporters arises from inverted-topology repeats. J Mol Biol **407**:698–715. 2011.

Reddy VS, Shlykov MA, Castillo R, Sun EI and Saier MH Jr. The major facilitator superfamily (MFS) revisited. FEBS J **279**:2022-35. 2012.

Saidijam M, Bettaney KE, Leng D, Ma P, Xu Z, Keen JN, Rutherford NG, Ward A, Henderson PJ, Szakonyi G, Ren Q, Paulsen IT, Nes I, Kroeger JK and Kolsto AB. The MFS efflux proteins of gram-positive and gram-negative bacteria. Adv Enzymol Relat Areas Mol Biol 77:147-166. 2011.

Saier MH Jr, Beatty JT, Goffeau A, Harley KT, Heijne WH, Huang SC, Jack DL, Jähn PS, Lew K, Liu J, Pao SS, Paulsen IT, Tseng TT and Virk PS. The major facilitator superfamily. J Mol Microbiol Biotechnol **1**:257-279. 1999.
Saier MH Jr. Families of transmembrane sugar transport proteins. Mol Microbiol **35**:699-710. 2000.

Smirnova I, Kasho V and Kaback HR. Lactose permease and the alternating access mechanism. Biochemistry **50**:9684–9693. 2011.

Smirnova I, Kasho V, Choe JY, Altenbach C, Hubbell WL and Kaback HR. Sugar binding induces an outward facing conformation of LacY. Proc Natl Acad Sci USA **104**:16504-16509.

Smirnova I, Kasho V, Sugihara J and Kaback HR. Opening the periplasmic cavity in lactose permease is the limiting step for sugar binding. Proc Natl Acad Sci USA **108**:15147-15151. 2011.

Smirnova I, Kasho V, Sugihara J and Kaback HR. Trp replacements for tightly interacting Gly-Gly pairs in LacY stabilize an outward-facing conformation. Proc Natl Acad Sci USA **110**:8876-8881. 2013

Sugihara J, Sun L, Yan N and Kaback HR. Dynamics of the L-fucose/H^+ symporter revealed by fluorescence spectroscopy. Proc Natl Acad Sci USA **109**:14847–14851. 2012.

The PyMOL Molecular Graphics System, Version 1.5.0.4 Schrödinger, LLC.

Yin Y, Jensen MØ, Tajkhorshid E and Schulten K. Sugar binding and protein conformational changes in lactose permease. Biophys J **91**:3972-3985. 2006.